Crystal Structures with a Chabazite Framework. III. Hydrated Ca-Chabazite at +20 and −150 °C

By J. V. Smith, C. R. Knowles and F. Rinaldi*

Department of the Geophysical Sciences, University of Chicago, Chicago 37, Illinois, U.S.A.

In part II, it was suggested that twinning of a low symmetry structure with rhombohedral geometry gave the best explanation of the biaxial optical properties and distorted electron-density peaks. The most likely cause of the low symmetry was ordering of the Si and Al atoms. The electron density map for data collected at −150 °C is almost identical with that for 20 °C, thus ruling out the possibility that the distorted peaks are caused by statistical occupancy of several sites. The ordered pattern of Si and Al atoms, which is most likely to be chemically stable, has triclinic symmetry. Mimetic twinning would result in near superposition of six peaks for each atom when calculations are based on rhombohedral symmetry. The six peaks for each calcium atom agree with the consesequence. Other atoms are represented by single peaks, but many of these are either distorted or yield large artificial temperature factors at both temperatures: this is interpreted as the result of near superposition of several atomic positions. The intensities do not exactly obey the mirror plane in $R\bar{3}m$, and this can be explained by imbalance between the twin units. Detailed analysis of peak shapes leads to a self-consistent set of coordinates in the triclinic cell $P\bar{1}$. The directions of the distortions from rhombohedral geometry form a sensible pattern resulting in more reasonable interatomic distances than those obtained from the averaged coordinates in $R\bar{3}m$. The only features of the proposed structure that cause concern are two short Ca–H_2O distances. Conclusive proof of the validity of the proposed structure can only come from X-ray analysis of an untwinned fragment.

Introduction

In the general introduction to this series of papers (Smith, 1962), the intention was stated of determining the atomic coordinates of different varieties of chabazite in order to provide a basis for interpretation of the chemical properties of this and other zeolites. The atomic coordinates of the alumino-silicate framework have been determined in straightforward fashion, but those of water molecules, chlorine molecules and calcium atoms have proven hard to define. In part II of this series (Smith, Rinaldi & Glasser, 1963), the structure of hydrated Ca-chabazite at room temperature was described. All calculations were based on the space group $R\bar{3}m$ indicated by the X-ray data. Peaks ascribed to one set of water molecules were strongly non-circular, while groups of six individual peaks were ascribed to calcium atoms. Optical examination of the chabazite had revealed a complex intergrowth of biaxial symmetry, probably the result of somewhat irregular twinning. After a long discussion of various possibilities, it was concluded that the most reasonable interpretation of all the data was that chabazite is of low symmetry (perhaps triclinic) but is geometrically rhombohedral. The electron density maps would then be the result of superposition of those for several (perhaps six) individual units. Ordering of the Si and Al atoms was thought to be the cause of the lower symmetry.

---

* Now at Montecatini, Istituto Donegani, Sezione Geochimica, Novarra, Italy.

A less likely explanation was that the water molecules and calcium atoms undergo strong anisotropic vibrations and/or random interchanges into several positions whose symmetry on a space-and-time average is rhombohedral. The biaxial optical properties would be ascribed to strain phenomena such as occur in quartz. In order to provide a test of these interpretations, it was decided to collect X-ray data at both room temperature and a low temperature. Ducros (1960) has shown from nuclear magnetic resonance studies of the protons in hydrated chabazite that the relaxation times for spin–spin interactions change markedly in the range +20 to −50 °C and only a little below −50 °C. Consequently it was decided that comparison of X-ray data at room temperature (20 °C) and at −150 °C would provide a significant evaluation of the effect of thermal motion.

Experimental

In part II, the electron density projection for crystal number 2 at room temperature was reproduced as Fig. 1(b). Unfortunately this crystal was lost and it became necessary to select another crystal for the comparison at room temperature and low temperature. Intensities for the $hk0$ reflections were collected for this new crystal of length 0·21 and cross-section 0·16 × 0·13 mm, mounted with the long direction parallel to the axis of a scintillation-counter Weissenberg goniometer. Absorption errors were trivial because of the use of quartz-monochromatized Mo $K\alpha$

radiation. After collection of data at room temperature, the crystal was cooled to at least -150 °C with the aid of a cryostat similar in design to that of Attard & Azaroff (1960). No attempt was made to control the jet of cold nitrogen gas to achieve a stability of better than 10 °C. The cell dimension a stayed constant at 9·45 Å, but the angle α increased from 94° 28' at room temperature to 94° 40' at low temperature. The widths and detailed shapes of the peaks obtained by rotating the crystal at constant angular velocity while the counter stayed stationary varied from reflection to reflection. Integrated intensities agreed closer than 10% across the centre of symmetry, but the reflections $hk0$ and $kh0$ which should be identical in $R\bar{3}m$ did not agree quite so well. Some of the extra variation might have come from mis-setting of the rotation axes, especially at low temperature for which the setting made at room temperature may not be strictly valid. However comparison of adjacent reflections in the reciprocal lattice showed variations somewhat greater than those across the center of symmetry, and the most likely explanation is that the symmetry is lower than $R\bar{3}m$. Because of the smallness of the effect, and the uncertainty of the measurements, the intensities of the reflections related by the mirror planes of $R\bar{3}m$ were averaged to give a single value.

The data for crystal 2, which has already been referred to, were obtained for a crystal of length 0·51 mm and cross-section 0·12 × 0·15 mm. The long axis was mounted parallel to that of the Weissenberg goniometer. Intensities were measured with a Geiger counter, using filters to stay in the linear region. Examination of the data given in Table 4 for the $h00$, $\bar{h}00$, $0k0$ and $0\bar{k}0$ reflections shows that there is better agreement across the centre of symmetry than across the supposed plane of symmetry. The discrepancy for the 10,0,0 group of reflections is too great to be caused by experimental error: two of the measurements are within the background fluctuations while two are eight times as great as the observable limit. Consequently there is no plane of symmetry relating these reflections. The evidence is not so clear for the other reflections, but there are several reflections with marked discrepancies. The electron density map for crystal 2 is shown in Fig. 4, and it will be shown later that the deviations from the plane of symmetry follow a consistent pattern. Consequently the evidence implies that $R\bar{3}m$ is only a pseudo space group of chabazite. The asymmetric shape of some of the intensity peaks obtained from the counter Weissenberg can be explained by small deviations from rhombohedral geometry.

Because of the difficulties of operation at low tem-
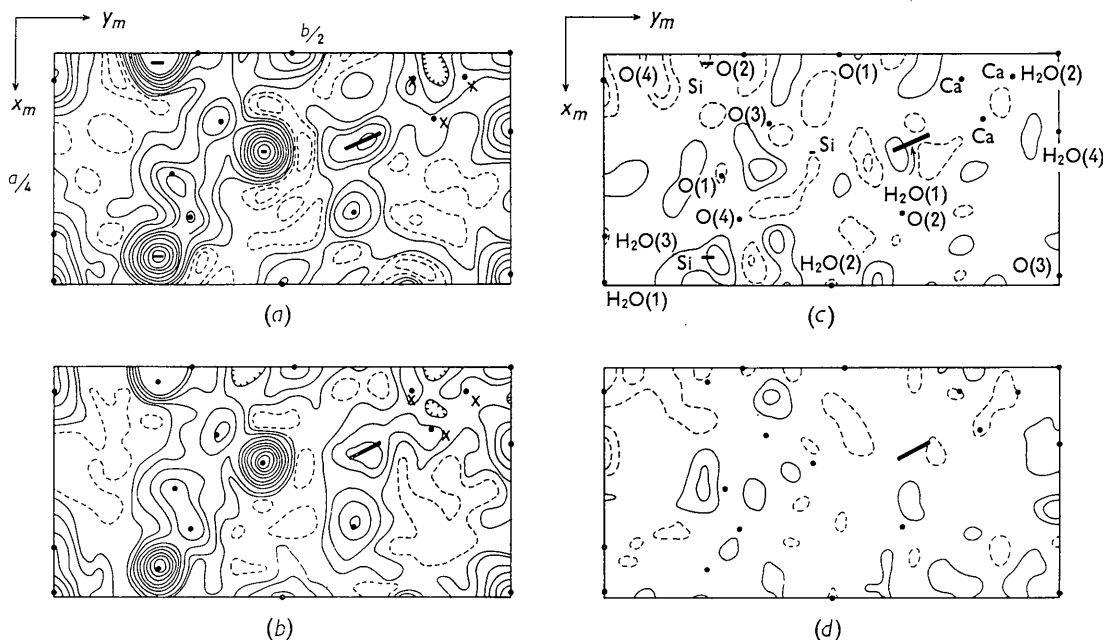
Fig. 1. The final F_o and F_o-F_c projections for the room-temperature (RT) and low-temperature (LT) structures of hydrated Ca-chabazite: (a) F_o at LT, (b) F_o at RT, (c) F_o-F_c at LT, (d) F_o-F_c at RT. The x_m and y_m axes are the long and short diagonals, respectively, of the rhombohedral cell projected down the c axis. Comparison of the atomic positions in Figs. 1 and 2 will clarify the relationship. The $H_2O(1)$ molecules in both structures are represented by two half-atoms joined together: a similar representation is given for the Si, Al atoms in the LT structure. The three crosses in both (a) and (b) are the peak positions for the $\frac{1}{4}$ Ca atoms that result from the averaged rhombohedral coordinates given in Table 3. The $\frac{1}{4}$ Ca peaks are displayed more clearly in the XRAC picture for crystal 2 (see Fig. 4). The contours in (a) and (b) are of equal spacing except at the centres of the Si, Al peaks, where alternate contours are omitted. For the Si, Al peaks at the upper left where overlapping occurs to give a very large peak, the central contours are omitted. The contours in (c) and (d) represent increments half as great as those in (a) and (b). For simplicity of drawing the x_m and y_m axes have been equalized.

perature, reflections with d less than 0·7 Å were not measured. Additional reflections were measured on both crystals at room temperature thus reducing the termination-of-series error which causes the diffraction rings around the Si, Al peaks in the F_o synthesis of the low-temperature structure (Fig. 1(a)).

Structure amplitudes and Fourier series were calculated for crystal 3 on an IBM 1620 computer by the use, respectively, of programs written by Prof. W. M. McIntyre of the University of Colorado and by Dr D. Van der Helm of the Institute for Cancer Research, Philadelphia. The rhombohedral axes were transformed into monoclinic axes so that $a_m = a_r + b_r$, $b_m = -a_r + b_r$, $c_m = c_r$. Refinement was carried out by successive $F_o - F_c$ syntheses, and the final F_o and $F_o - F_c$ syntheses referred to the axes a_m and b_m are shown in Fig. 1. Each atomic peak was adjusted separately even though the rhombohedral symmetry required relations between coordinates of peaks belonging to the same atomic group. Overlapping of several peaks resulted in only one determination for some parameters, but most coordinates were determined independently from two separate peaks.

For the program of McIntyre, the approximation $A \exp(-a \sin^2 \theta) + B \exp(-b \sin^2 \theta)$ is used for the form factor (Vand, Eiland & Pepinsky, 1957). In the calculations for chabazite, half-ionized atoms were used, yielding the following values of A, a, B and b for the (Si, Al), Ca and O atoms, respectively: 7·80, 2·40, 4·03, 28·2; 10·55, 1·98, 8·45, 32·9; 3·46, 3·29, 5·54, 37·2. Water molecules were assigned the scatter-

ing factor for half-ionized oxygen. The H_2O peaks at both temperatures and the Si, Al peaks at low temperature were elliptical, and were approximated by two half atoms.

Table 2. *Parameters for final calculation of structure factors for low-temperature structure using the monoclinic unit cell*

		x	y	B
Si, Al	$\lbrace$	0·2192	0·1070	0·2
		0·2192	0·1190	
	$\lbrace$	0·0100	0·1078	0·2
		0·0100	0·1198	
	$\lbrace$	0·1050	0·2265	0·2
		0·1050	0·2305	
O(1)		0·1295	0·1295	1·8
		0·0000	0·2590	1·7
O(2)		0·1720	0·3280	1·7
		0·0000	0·1560	1·7
O(3)		0·0750	0·1810	1·8
		0·2600	0·0000	1·8
O(4)		0·1770	0·1490	1·9
		0·0270	0·0000	1·9
Ca		0·025	0·450	0·6
		0·027	0·394	0·6
		0·070	0·417	0·6
$H_2O(1)$	$\lbrace$	0·102	0·319	1·7
		0·085	0·357	
		0·247	0·000	1·7
$H_2O(2)$		0·000	0·500	2·0
$H_2O(3)$		0·197	0·000	2·0
$H_2O(4)$		0·084	0·500	1·9

Bracketed values are the coordinates for two half-atoms used to approximate elliptical peaks.

Tables 1 and 2 contain the positions of the peaks referred to monoclinic axes, while Table 3 contains the atomic coordinates transformed to rhombohedral axes and averaged. Fig. 2 shows the positions of the atoms in the rhombohedral cell. Table 4 contains the observed and calculated structure amplitudes. Excluding the unobserved reflections, the discrepancy index is 0·12 at room temperature and 0·147 at low temperature; when the extra reflections are included the index rises to 0·16 and 0·154, respectively. The large increase in the room-temperature discrepancy index as the unobserved reflections are added results chiefly from the inclusion of unobserved high-order reflections.

Reliable estimates of the accuracy of the atomic parameters are hard to make. Perhaps the best estimate of the atomic coordinates is obtained by comparing the pairs of values obtained from different peaks. For the Si, Al atoms in the room-temperature structure the difference between the two values for x_r, y_r and z_r are 0·0022, 0·0003 and 0·0001, while for the low-temperature structure they are 0·0024, 0·0003 and 0·0013. For the oxygen atoms and water molecules the discrepancies are larger. The errors for the low-

Table 1. *Parameters for final calculation of structure factors for room-temperature structure using the monoclinic unit cell*

		x	y	B
Si, Al		0·2192	0·1137	0·5
		0·0105	0·1138	0·5
		0·1044	0·2288	0·5
O(1)		0·1320	0·1320	2·0
		0·0000	0·2640	2·0
O(2)		0·1730	0·3270	2·0
		0·0000	0·1520	2·0
O(3)		0·0740	0·1780	2·0
		0·2550	0·0000	2·0
O(4)		0·1750	0·1490	2·0
		0·0255	0·0000	2·0
Ca		0·027	0·450	1·5
		0·027	0·390	1·5
		0·068	0·414	1·5
$H_2O(1)$	$\lbrace$	0·100	0·324	2·5
		0·082	0·357	2·5
		0·244	0·000	2·5
$H_2O(2)$		0·000	0·500	2·8
$H_2O(3)$		0·194	0·000	1·5
$H_2O(4)$		0·084	0·500	1·5

Bracketed values are the coordinates for two half-atoms used to approximate elliptical peaks.

Fig. 2. The atomic coordinates shown in projection down the rhombohedral z axis. The heights expressed as a percentage of c are shown in the circles for the oxygen atoms and water molecules, and near the solid circles and squares for the Si, Al and Ca atoms, respectively. Because of the elongated peaks in Fig. 1 for the $H_2O(1)$ molecules, thick lines are used, whose ends are at the coordinates of the two half-atoms used as an approximation. The six positions for the two Ca atoms are shown; the two positions chosen for the triclinic unit cell are shown by heavier dots. The Si, Al–O bond lengths are shown at the lower right, and those bonds that form an eight-membered ring are also shown.

Table 3. Coordinates based on $R\bar{3}m$

	Multiplicity	Low temperature			Room temperature		
		x	y	z	x	y	z
Si, Al	12	0·1050	0·3328	0·8764	0·1044	0·3330	0·8756
O(1)	6	0·259	−0·259	0·000	0·264	−0·264	0·000
O(2)	6	0·156	−0·156	0·500	0·153	−0·153	0·500
O(3)	6	0·258	0·258	0·894	0·253	0·253	0·896
O(4)	6	0·027	0·027	0·326	0·026	0·026	0·324
$H_2O(1)$	6	0·246	0·246	0·568	0·244	0·244	0·573
$H_2O(2)$	3	0·500	0·500	0·000	0·500	0·500	0·000
$H_2O(3)$	2	0·197	0·197	0·197	0·194	0·194	0·194
$H_2O(4)$	2	0·416	0·416	0·416	0·416	0·416	0·416
$\frac{1}{3}$ Ca	12	0·357	0·494	0·577	0·354	0·498	0·575

See text for derivation of these coordinates from the data in Tables 1 and 2.

temperature structure are greater than those for the room-temperature structure because of the smaller number of observed reflections for the former. Detailed analysis is not warranted because of un-

certainties of the symmetry, and it is sufficient to deduce that the standard errors of the Si, Al–O and O–O bond lengths should be not greater than 0·03 and 0·04 Å, respectively. These values appear quite

Table 4. *Observed and calculated structure amplitudes for hydrated Ca chabazite at room temperature* (RT) *and low temperature* (LT)

Crystal 3 / Crystal 2 (RT)

		Crystal 3 RT		Crystal 3 LT		Crystal 2 (RT) 1	2	3	4
h	k	Fo	Fc	Fo	Fc	Fo	Fo	Fo	Fo
1	0	42	+48	44	+47	36	34	36	35
2		24	-21	25	-22	24	23	24	22
3		3	-5	6	-8	4	3	4	1
4		19	-19	23	-20	21	25	21	18
5		64	-66	67	-67	64	61	64	60
6		10	+7	6	+7	10	8	10	8
7		21	+17	19	+17	16	18	16	19
8		48	+48	50	+51	43	48	43	50
9		55	+55	61	+57	53	51	53	52
10		0	+7	6	+5	7	3	7	2
11		14	-12	13	-12	10	10	12	10
12		14	+13	15	+16	12	14	12	14
13		32	-32	33	-37	27	25	27	28
14		19	-18			18	17	18	18
15		7	+8			6	7	6	6
1	1	22	+39	25	+37	23			
2		11	-9	15	-7	11	9		
3		71	+77	74	+79	65	64		
4		3	-5	10	-10	2	5		
5		65	-61	61	-62	68	60		
6		14	-13	8	-11	13	11		
7		35	-31	34	-31	31	20		
8		4	-5	6	-7	3	6		
9		32	+27	32	+29	30	24		
10		0	+3	7	+4	3	3		
11		0	-2	7	-3	3	3		
12		9	+9	11	+12	10	9		
13		12	-15	15	-14	12	12		
14		13	-19			14	10		
2	2	45	+48	47	+47	46			
3		64	+67	58	+64	67	62		
4		4	+8	8	+9	3	3		
5		3	-4	0	+0	3	5		
6		0	+6	0	+6	2	2		
7		36	-34	36	-38	32	32		
8		26	-19	22	-22	24	21		
9		11	-13	10	-12	10	9		
10		0	+1	0	-0	5	2		
11		0	+1	0	+0	5	3		
12		15	+18	20	+20	13	13		
13		14	+13	18	+15	14	12		
14		0	+7			3	6		
15		0	-5			4	6		
16		8	-9			5	7		
3	3	3	-2	5	-4	2			
4		18	+14	16	+15	17	15		
5		5	-3	6	-5	2	4		
6		40	-36	44	-42	42	43		
7		8	-8	11	-10	4	4		
8		5	+6	8	+8	6	7		
9		15	+17	16	+18	13	13		
10		11	+11	12	+10	10	15		
11		13	+12	18	+12	13	10		
12		11	-12	20	-13	14	10		
13		nm	nc			5	4		
14		0	-6			3	4		
15		10	-8			8	10		
4	4	53	+45	61	+50	59			
5		42	+43	46	+44	44	46		
6		29	-28	30	-28	29	26		
7		3	-3	6	-4	4	2		
8		5	+4	7	+4	2	7		
9		34	-31	39	-33	30	31		
10		4	-5	10	-6	7	3		
11		16	+17	18	+19	10	15		
12		4	-5	8	-4	8	12		

Middle section

h	k	RT Fo	Fc	LT Fo	Fc	Fo	Fo
5	5	54	+60	66	+64	58	
6		9	-5	9	-5	10	10
7		2	-7	8	-8	6	3
8		16	-19	17	-20	14	15
9		45	-45	46	-48	42	40
10		13	-12	4	-12	9	10
11		9	+10	nm	+10	7	6
12		nm	nc			4	4
13		13	+12			13	11
14		16	+17			17	12
6	6	25	+28	24	+29	25	
7		7	+13	13	+12	14	14
8		19	+17	22	+20	19	16
9		3	-6	11	-8	6	4
10		0	+1	0	+1	4	4
11		3	-9	nm	-13	3	3
12		nm	nc	17	-16	9	14
13		10	-8			11	8
7	7	12	+7	4	+6	9	
8		9	+8	12	+11	8	8
9		3	+3	0	+2	8	4
10		4	-8	nm	-11	3	3
11		9	-11			9	7
12		7	-4			6	7
8	8	10	-8	nm	-9	8	
9		4	+10	nm	+12	4	7
10		nm	nc			11	12
11		nm	nc			4	3
12		18	+17			18	15
9	9	22	+21	24	+25	22	
10		0	+10			3	4
11		9	-10			9	6
12		4	+2			3	5
13		9	-8			9	3
14		12	-13			11	3
1	$\bar{1}$	32	-33	27	-34	31	
2		79	-70	74	-73	82	73
3		6	-8	0	-5	3	1
4		12	+8	13	+11	3	9
5		15	-15	16	-15	15	14
6		69	+66	57	+63	68	67
7		8	+4	8	+4	6	3
8		7	+5	7	+8	6	2
9		12	+8	11	+9	11	12
10		16	-15	17	-17	16	15
11		10	-10	12	-13	11	10
12		14	+11	16	+12	16	15
13		0	+1	0	+1	4	3
14		0	-1			3	3
15		15	+11			14	---
2	$\bar{2}$	60	-54	55	-49	51	
3		21	-18	15	-16	19	13
4		18	-20	15	-22	16	17
5		9	+10	11	+11	8	8
6		48	+50	53	+51	53	45
7		31	+25	26	+22	28	28
8		8	-8	11	-11	7	8
9		0	-10	7	-9	2	3
10		16	-18	15	-17	14	16
11		18	-17	14	-13	13	12
12		12	-11	12	-10	10	9
13		7	-8	11	-9	8	7

Right section

h	k	RT Fo	Fc	LT Fo	Fc	Fo	Fo
3	$\bar{3}$	59	+50	50	+43	57	
4		15	+19	13	+14	13	14
5		4	-4	7	-6	5	7
6		18	-15	16	-17	14	14
7		43	+43	43	+39	43	37
8		27	+27	29	+28	23	23
9		10	-16	10	-12	5	6
10		8	+11	11	+13	4	2
11		0	-6	8	-8	3	3
12		20	-20	22	-24	18	18
13		0	-2	12	-4	5	3
14		0	+0			3	6
15		0	+1			3	3
16		6	+9			6	5
4	$\bar{4}$	110	+108	100	+104	100	
5		50	+51	53	+52	53	48
6		2	-2	0	-2	3	2
7		33	+33	33	+32	30	31
8		20	-15	19	-6	17	17
9		34	-39	43	-37	42	39
10		9	-12	11	-15	10	10
11		7	+7	9	+9	8	7
12		0	+6	6	+8	7	3
13		31	+30	29	+29	26	25
14		17	+23			16	15
5	$\bar{5}$	33	+27	36	+30	30	
6		24	-23	21	-24	23	20
7		3	-5	5	-5	2	2
8		19	-19	20	-17	15	17
9		30	-30	22	-30	27	15
10		16	+16	17	+16	15	15
11		0	+3	0	+1	3	3
12		7	-8	9	-7	9	6
13		18	+16	20	+19	17	15
14		8	+5			11	3
6	$\bar{6}$	0	+2	6	+5	8	
7		10	-8	9	-7	3	8
8		4	-5	9	-6	2	2
9		0	-1	0	+1	2	2
10		25	+22	22	+21	24	22
11		12	+6	7	+0	10	11
12		0	+1	0	+3	3	3
13		nm	nc			9	4
14		0	-5			3	3
15		14	-12			13	13
7	$\bar{7}$	29	-20	27	-20	21	
8		13	-13	15	-14	11	12
9		0	-3	9	-2	2	2
10		3	+4	4	+4	7	3
11		19	+21	13	+18	16	12
12		25	+25	12	+22	21	20
8	$\bar{8}$	21	+18	16	+18	17	
9		25	+24	19	+24	21	23
10		4	+5	0	+4	3	3
9	$\bar{9}$	45	+48	31	+45	41	
10		0	+1			3	6
11		0	-3			3	3
12		0	-9			3	3
13		18	-27			14	17

nm   not measured   nc   not calculated

For crystal 2, columns 1 and 2 are for pairs of reflections related by the plane of symmetry.
Columns 3 and 4 are related to columns 1 and 2, respectively, by a centre of symmetry.

reasonable, for the observed Si, Al–O distances range only from 1·64 to 1·66 Å in the room-temperature structure and from 1·63 to 1·67 Å at low temperature.

There is even less certainty about the significance of the artificial temperature factors. The actual value is affected by the assumed value of the atomic scattering factor. In addition, the use of half-atoms complicates the situation: furthermore, if the electron-density maps are the sum of six maps for a triclinic structure, the whole basis of the use of artificial temperature factors is questionable. Nevertheless, to the level of approximation used here, the average temperature factor for all the atoms is slightly, but significantly, changed at low temperature. The clearest evidence of this is for the Si, Al atoms for which it was necessary to use two half-atoms to explain the elliptical peaks at low temperature, whereas the peaks were circular at room temperature.

A special word is necessary about the calcium atoms. As described in detail in part II, six small peaks are ascribed to each of the two calcium atoms (see Fig. 1 and 2 of this paper). The peaks might result either from two calcium atoms uniformly distributed on a space-and-time average between a general position of twelvefold multiplicity in $R\bar{3}m$, or from two calcium atoms in a general position in another space

group of lower symmetry (perhaps $P\bar{1}$), repeated six times by twinning to mimic the symmetry of $R\bar{3}m$. In either case, the coordinates of the three peaks should be related in pairs by the triad axis. Table 3 shows the averaged coordinates in the rhombohedral cell, and Fig. 1 shows the Ca peak positions calculated from these averaged coordinates. It may be seen that the discrepancies between the observed and calculated peak positions average 0·1 Å in the room-temperature synthesis and 0·2 Å in the low-temperature structure. These discrepancies, although large, are possible when the low peak heights and the likelihood of a few incorrect signs for the weaker reflections are taken into account.

Table 5. *Interatomic distances for coordinates based on $R\bar{3}m$*

The distances to the calcium atom were calculated with coordinates of (0·355, 0·496, 0·576) for the calcium atom, and averages for the low-temperature (LT) and room-temperature (RT) determinations of the coordinates of the other atoms

	RT Structure	LT Structure
Si–O(1)	1·64 Å	1·63 Å
–O(2)	1·66	1·67
–O(3)	1·65	1·66
–O(4)	1·66	1·66
O(1)–O(2)	2·66	2·68
–O(3)	2·74	2·73
–O(4)	2·74	2·72
O(2)–O(3)	2·64	2·62
–O(4)	2·74	2·77
O(3)–O(4)	2·66	2·70
$H_2O(1)$–$H_2O(4)$	2·79	2·75
–O(1)	2·88	2·95
–O(3)	3·03	3·06
–O(4)	3·45	3·40
–$H_2O(3)$	3·57	3·48
–$H_2O(2)$	3·54	3·53
–O(2)	3·60	3·60
–O(2')	3·76	3·81
$H_2O(2)$–O(1)	3·27	3·35
–O(2)	3·48	3·46
–$H_2O(1)$	3·54	3·53
$H_2O(3)$–O(4)	2·60	2·61
–O(3)	3·00	3·06
–$H_2O(4)$	3·34	3·28
–$H_2O(1)$	3·57	3·48
$H_2O(4)$–$H_2O(4')$	2·53	2·52
–$H_2O(1)$	2·79	2·75
–$H_2O(3)$	3·34	3·28
Ca–$H_2O(4)$	1·79	
–$H_2O(4')$	2·25	
–$H_2O(1)$	2·51	
–$H_2O(1')$	2·87	
–Ca'	3·22	
–O(2)	3·30	
–$H_2O(1'')$	3·36	
–$H_2O(2)$	3·38	

Table 5 lists the interatomic distances calculated from the averaged rhombohedral coordinates of Table 3. Because of the low accuracy of the coor-

dinates for the calcium atom, averaged distances for the two structures are given when the distance involves this atom.

The electron-density projection for crystal 2 (Fig. 4) was obtained by taking the data from Table 4 of this paper, using the signs from Table 3 of part II, and photographing the image obtained on the XRAC analogue computer. No further calculations have been made on these data, but it may be seen that the peaks are consistent with the coordinates obtained from the data of crystal 3. The reflections were not averaged in this calculation, so there is no diagonal mirror plane. Deviations from a centre of symmetry are caused merely by tolerances in the electronic components of XRAC.

Discussion

The two structures for crystal 3 at room temperature and low temperature are extremely close, and only a few parameters change by amounts greater than the experimental error. Perhaps the most certain indicator of a change is the interaxial angle α which moves $12 \pm 5'$. The atomic coordinates of the two structures are so close that no certain deductions of change can be made. On the average, the artificial temperature factors fall by 0·3, but the individual values show considerable variation with two actually increasing. The evaluation of the temperature factors is complicated by non-circular peaks, especially for $H_2O(1)$ at both temperatures and for (Si, Al) at low temperature. The most reasonable interpretation of the smallness of the change with temperature, and the consequent largeness of the artificial temperature factor at low temperature is that part of the artificial temperature factor arises not from thermal motion but from averaging of more than one set of atomic peaks. This conclusion is in harmony with the suggestion that chabazite is dimensionally rhombohedral but actually of lower symmetry.

The most likely cause for a lower symmetry is ordering of the Si and Al atoms (as suggested in part II), but other possibilities such as change of inter-bond angles from those in symmetrical configurations in order to reduce the internal energy cannot be ruled out. It is not possible to use the present data to determine whether a scheme of ordering occurs, but it is possible to deduce a preferred scheme of ordering from stability considerations. Study of feldspar and other minerals has shown that in alumino-silicate frameworks, Al atoms are distributed so that they are not linked to the same oxygen atom. In anorthite (Megaw, Kempster & Radoslovich, 1962), gismondine (Fischer, 1962), kalsilite (Perrotta & Smith, in preparation) where the Si/Al ratio is unity, the avoidance rule suggests that Si and Al atoms alternate, and this indeed is what is found. In chabazite, which has a ratio near 2, the situation is more complicated. No evidence has been obtained for a superstructure in

(a)   (b)   (c)
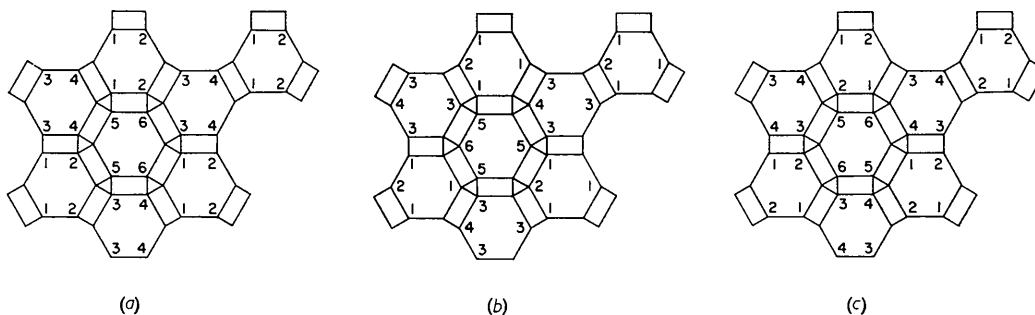
Fig. 3. The three possible ordered arrangements of Si and Al atoms in chabazite which do not have two Al atoms of any one
hexagonal prism sharing an oxygen atom. In (a) and (b), Al atoms do not share oxygen atoms in the four-membered rings
joining the prisms, but in (c), oxygen atoms are shared in these rings. Arrangements (a) and (b) have symmetry $P\bar{1}$ and $P1$,
respectively. The diagrams are highly schematic representations of the structure viewed down the pseudo-triad axis. The
Si, Al atoms lie at the intersection of the lines, and the heights of the intersections are expressed by the numbers 1 to 6. The
hexagonal prisms are formed from pairs of rings at heights 1 and 2 or 3 and 4 or 5 and 6, and are joined by inclined four-
membered rings at heights 2 and 3 or 4 and 5 or 6 and 7 (7 is the repeat of 1). The positions of Al atoms are given by assigning
a height: absence of a height at an intersection implies the occurrence of an Si atom. In (a), each hexagonal ring contains
two Al atoms, whereas in (b) the rings alternately have three and one.

chabazite, so it can be assumed that the 9·5 Å repeat
is valid for all three axes. Fig. 3 shows three of the
ways in which the 8 Si and 4 Al atoms may be placed
in an ordered configuration in the unit cell. In (a)
and (c), 2 Al atoms are placed in each of the two
hexagonal rings which form the hexagonal prisms
that lie one at each corner of the unit cell, while in
(b) three are placed alternately around one of the
rings and only one in the other. Examination of (c)
shows that Al atoms share oxygen atoms in the
four-membered rings which link together the hexagonal
prisms. There are no shared oxygen atoms in either
(a) or (b), but the former is more likely because it
has a more uniform arrangement of Al atoms.
Examination of structures such as spinel and corun-
dum, where cations occupy only a fraction of the
possible interstices, shows that the chosen sites are
arranged as uniformly as possible, or in other words,
the average distance between cations is as great as
possible. This is an obvious condition for stability
in purely ionic structures. Applying this idea to the
arrangement of Al atoms in the chabazite framework,
the arrangement (a) is the one preferred here. The
symmetry of (a) is centred, $P\bar{1}$, while that of (b) is
uncentred $P1$.

The only detailed optical study of chabazite so
far carried out was by Majer (1953) who found that
his specimen was optically triclinic and sextuply
twinned. This is fully consistent with the ordering
scheme proposed here, for the symmetry elements of
$R\bar{3}m$ would become twin elements operating on the
$P\bar{1}$ structure thus yielding sixfold twinning. Whether
the twinning is primary or secondary is a matter for
further investigation, the results of which might
provide evidence on whether chabazite formed with
an ordered or a disordered pattern of Si and Al atoms.

Sextuple twinning of a triclinic structure would
result in six peaks for each atom in the electron

density maps, except for atoms lying on twin
elements, which would yield a smaller number of
peaks. There are indeed six peaks ascribed to each
calcium atom, and these peaks obey, within the
large experimental error, the permutation of coor-
dinates required by the triad axis. The other atoms
give single peaks, but the large value of the artificial
temperature factor at low temperature and the
elongation of the peaks for the $H_2O(1)$ molecules are
indicative of averaging of more than one atomic
position. Furthermore, in the F_o projection of crystal 2
(Fig. 4) for which the intensities for the $hk0$ and $kh0$
reflections were not averaged, the peaks for the
$H_2O(1)$ molecule show a threefold structure, while
those for the $H_2O(4)$ molecule display distortion in
at least three directions.

Examination can be made of the artificial tempera-
ture factors in order to estimate the amounts of atomic
displacements. The well-known formula $B = 8\pi^2\overline{u_s^2}$
was derived by Debye & Waller to relate the isotropic
temperature factor $\exp(-B\sin^2\theta/\lambda^2)$ to the mean
of independent Gaussian vibrations $\overline{u_s^2}$. Obviously
this theory cannot apply accurately to the displace-
ments caused by twinning, but it can be used to give
an approximation to them. At low temperatures,
the thermal motion will be reduced, so much of the
observed temperature factor can be ascribed to dis-
placements caused by twinning.

The B values of the Si, Al atoms are very small (0·2);
however, it was necessary to use half-atoms displaced
by 0·04 to 0·10 Å to take account of the elliptical
peaks. The oxygen atoms have an average B of 1·8
which corresponds to $\overline{u_s^2}$ of 0·023 Å². Smith & Bailey
(1963) have shown that in framework structures the
Al–O distance is 0·14 Å longer than the Si–O bond
length. If the Si and Al atoms occupy positions exactly
related by symmetry, the O atoms must deviate by

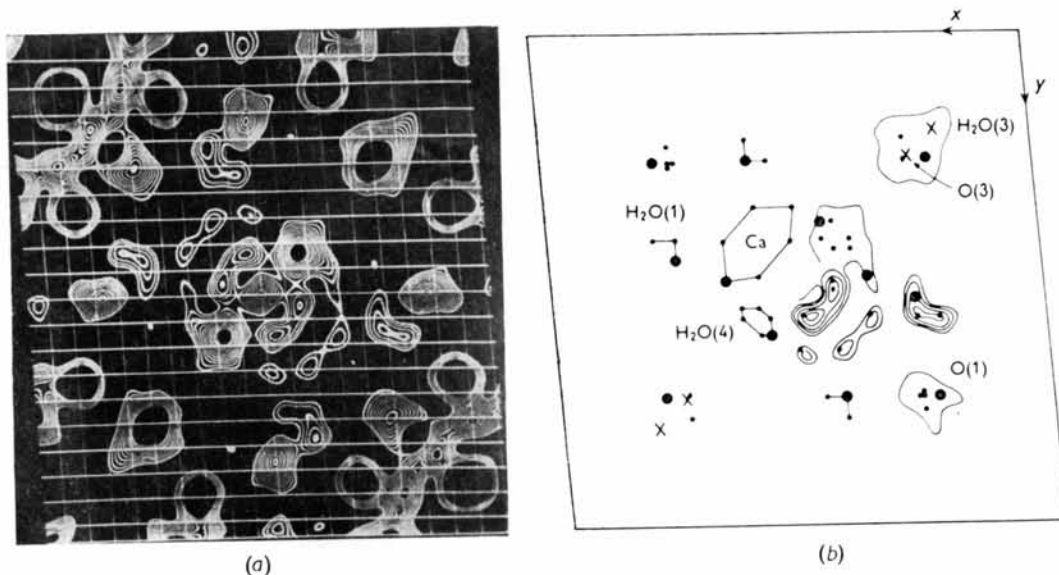(a)   (b)

Fig. 4. (a) F_o projection down the rhombohedral z axis of crystal 2 using unaveraged $hk0$ and $kh0$ amplitudes summed by XRAC. (b) Proposed positions of Ca and O(1) atoms and of $H_2O(1)$ molecules in the twinned triclinic structure. The large filled circles show the atomic positions for one of the twin units while the small ones are for the five units related by the mimetic twinning. For Ca and $H_2O(4)$, six peaks are shown joined to form hexagons on one side of the centre of symmetry, and are unlinked on the other side. For $H_2O(1)$ overlapping of positions leaves only three circles. One set of $H_2O(1)$ positions overlap with those for O(3) and $H_2O(3)$ shown by crosses. Overlapping of two positions leaves only five circles for the O(1) atom. Several contours are copied from (a) to permit easy comparison between the two diagrams.

at least 0·07 Å from the ideal sites. The calculated value of $\overline{u_s^2}$ (0·005) is not greater than the observed value, which is satisfactory because the difference can be ascribed to residual thermal motion and to additional distortion of the alumino-silicate framework.

The B values for $H_2O(2)$, $H_2O(3)$ and $H_2O(4)$ molecules are slightly greater than those of the oxygen atoms. Assuming that the atomic scattering factor for half-ionized oxygen represents the water molecules satisfactorily, the B values of 2·0 require that $\overline{u_s^2} = 0·025$ Å². For $H_2O(1)$ the peaks were so elliptical that it was necessary to replace the isotropic scattering factor by that for two half-atoms displaced by about 0·5 Å, in addition to using a B of 1·7. The above values would indicate mean atomic displacements from an average position for $H_2O(1)$, of 0·3 Å with the major displacement being along the line joining the two half-atoms; and for the other water molecules of 0·1 to 0·2 Å, isotropically distributed.

The consistency of the X-ray and optical evidence for triclinic symmetry encouraged an analysis of the peaks in order to attempt a determination of the triclinic coordinates. Because all six peaks ascribed to each calcium atom are resolved, the rhombohedral coordinates in Table 3 should be the same as those in the triclinic unit cell. As the most reasonable ordered configuration of Al and Si atoms is centred, it will be assumed that the two Ca atoms are related by a centre of symmetry. Examination of the $H_2O(1)$ peaks obtained for crystal 2 at room temperature

(Fig. 4) shows that they are distorted into a triplet pattern. (The fine detail of the peaks would not be revealed by the usual calculation of electron density at points on a 100×100 or a 120×120 grid. An analogue computer such as XRAC is particularly good for study of peak shapes because of the continuous nature of the presented information). The x, y coordinates of the three peaks are 0·215, 0·585; 0·26, 0·575; 0·26, 0·54. In a $P\bar{1}$ cell, $H_2O(1)$ will be represented by three pairs of atoms at $\pm(x_iy_iz_i)$ with $i = 1$, 2 or 3. Mimetic rhombohedral twinning will permute these coordinates to give

$$\pm[(x_iy_iz_i)(z_ix_iy_i)(y_iz_ix_i)(x_iz_iy_i)(y_ix_iz_i)(z_iy_ix_i)].$$

Each peak for $H_2O(1)$ will be combined from six peaks. However only three peaks are seen, and this can only be the result of equality or near-equality of some of the triclinic coordinates. As may be seen from Fig. 4, the triclinic coordinates

$$\pm[(0·42, 0·74, 0·785)(0·215, 0·26, 0·58)(0·26, 0·54, 0·26)]$$

give an adequate explanation of the observed peak shapes for crystal number 2.

The validity of the coordinates was then tested by calculating interatomic distances. Each Ca atom has three near $H_2O(1)$ neighbours. Before removal of the $H_2O(1)$ molecules from the average rhombohedral coordinates of 0·245, 0·245, 0·570, the distances were 2·5, 2·9 and 3·3 Å. After movement to the above triclinic coordinates, the distances became 2·5, 2·7 and 3·1 Å.

Each Ca atom is close to two $H_2O(4)$ molecules at $\pm (0.416, 0.416, 0.416)$ giving distances of 1.8 and 2.25 Å. These distances are very low, especially the first one. The peak for the $H_2O(4)$ molecule in Fig. 4 is reasonably circular but the outer contours have a cog shape. Displacement of the $H_2O(4)$ molecules to $\pm (0.440, 0.420, 0.385)$, which give an average coordinate of $\pm (0.415, 0.415, 0.415)$ in the rhombohedral cell, changed the Ca–$H_2O(4)$ distances from 1.8 and 2.25 to 2.0_3 and 2.1_3. These displacements do not give an exact explanation of the shape of the peak in Fig. 4 but the representation is reasonably close. The amount of displacement is within the observed value of $\overline{u_s^2}$ deduced from the artificial temperature factor.

The displacements of $H_2O(1)$ molecules to $(0.42, 0.74, 0.785)$ and $(0.26, 0.54, 0.26)$ change the distances to the O(1) atom at $(0.26, 0.74, 0.00)$ so that they now differ by 0.8 Å. Consequently it would be expected that the O(1) atom would move to equalize the distances. The predicted movement of the O(1) atom is in accordance with the observed distortion of the peak in Fig. 4. Similar movements are postulated for the other O(1) atoms and these would require movements of other atoms in the tetrahedral framework. However the resolution of peaks is not good enough to permit further investigation of possible displacements.

A test of the displacements can be made by examining the heights of the peaks. Of the six peaks for the Ca atom in Fig. 4, two are considerably larger than the other four, which can be explained by imbalance between the twin units. Examination of the peaks for the $H_2O(1)$ molecules shows that the highest part fits with the displacements expected for the two stronger twin units. This agreement might be coincidental, but provides one further piece of evidence to confirm the suggestion of a twinned triclinic structure.

The postulated triclinic coordinates are listed in Table 6, and the vectors from the Ca, $H_2O(1)$, $H_2O(3)$ and $H_2O(4)$ positions to all atoms or molecules not more than 3.2 Å away are shown in Fig. 5. The Ca atoms lie in pentahedra of water molecules at distances of 2.0, 2.1, 2.5, 2.7 and 3.1 Å, which share an edge of length 2.7 Å. The $H_2O(1)$ molecules are of three types; (a) has a Ca neighbour at 2.5 Å, a water molecule at 2.6 Å and three oxygen atoms at 2.6, 2.7 and 3.0 Å; (b) has a Ca neighbour at 2.7 Å, a water molecule at

2.6 Å and three oxygen atoms at 3.0, 3.1 and 3.4 Å. Each $H_2O(4)$ molecule has two Ca neighbours at 2.0 and 2.1 Å, and four H_2O molecules at 2.4, 2.6, 2.6 and 2.7 Å. The $H_2O(3)$ molecules near the centres of the hexagonal rings have three oxygen atoms as neighbours at 2.6 Å and three more at 3.0 Å. The $H_2O(2)$ molecules at the centres of the octagonal rings are over 3.2 Å away from all neighbours, and are not shown on Fig. 5. (Actually Fig. 4 gives doubled peaks for the $H_2O(2)$ molecules at $0, \frac{1}{2}$ and $\frac{1}{2}, 0$. It is possible that the molecules move away from the centres of the octagonal rings to permit shortening of some of the interatomic distances: such movements require loss of the centre of symmetry, unless carried out on a statistical basis).
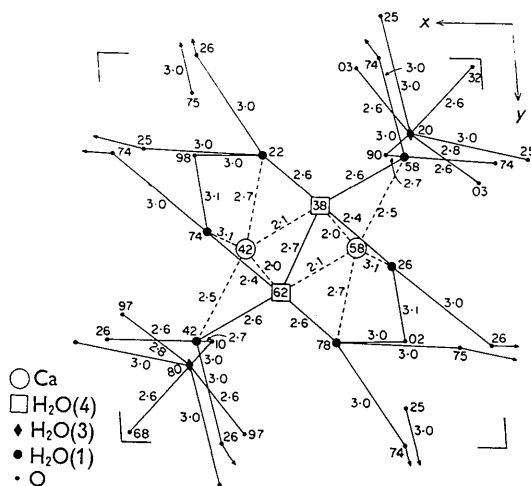

Fig. 5. Interatomic distances from Ca atoms and H_2O molecules for the proposed triclinic structure shown in projection down the z axis. The heights of the atoms are shown as percentages of the c spacing. The atomic coordinates for Ca, O(1), $H_2O(1)$ and $H_2O(4)$ are listed in Table 6, and for the other atoms in Table 3.

Typical Ca–O distances are around 2.4 Å, but values as low as 2.3 Å have been reported: in anorthite (Megaw, Kempster & Radoslovich, 1962) the shortest distances are 2.28, 2.32, 2.33 and 2.35 Å (± 0.004); in gypsum (Atoji & Rundle, 1958) the distances are 2.34, 2.35, 2.58, 2.59 Å; in afwillite (Megaw, 1952) Ca–O distances are 2.30 Å upwards (all ± 0.04). Consequently two of the Ca–H_2O distances in chabazite (those at 2.0_3 and 2.1_3) are considerably lower than in the above-named structures, and indeed appear to be too low. However a very low value of 2.03 Å for the distance Na–H_2O in a 38% aqueous solution of NaOH has been reported by Devik, Finbak & Rønning (1944) from analysis of radial distribution curves: moreover, Howell (1960) reports Na–O distances of 2.14 and 2.27 Å in dehydrated Type A synthetic zeolite. As the Na–O and Ca–O distances in crystals are closely similar this would suggest that rather low distances may be

Table 6. *Proposed atomic coordinates based on $P\bar{1}$*

Atom	x	y	z
Ca	0.44	0.42	0.385
$H_2O(1)$	0.215	0.26	0.58
	0.26	0.54	0.26
	0.42	0.74	0.785
$H_2O(4)$	0.44	0.42	0.385
O(1)	0.23	0.74	0.02
	0.26	0.00	0.74
	0.98	0.27	0.74

possible for Ca–O bonds. It is possible that the Ca–H_2O distances in chabazite are too low because of errors of locations of the Ca atom and water molecules; earlier evidence was presented that the calcium atoms were not located to better than 0·1 to 0·2 Å.

Wells (1962) has given a general summary of hydrogen bonding and of water and hydrates which is very useful for the present purpose of determining whether the coordination in the proposed triclinic structure is reasonable. The H_2O–H_2O distances in the proposed triclinic structure of chabazite are quite reasonable, for the observed range from 2·4 Å upwards is the same as that found in other hydrogen-bonded structures. Examination of the environment of water molecules in other structures shows that in those where the elements other than water are free to move, the water molecules adopt a tetrahedral environment. As the structural needs of the other elements become more demanding, the environments of the water molecules deviate more and more from tetrahedral patterns. In the zeolite harmotome (Sadanaga, Marumo & Takéuchi, 1961) all distances to the water molecules are long, usually over 3 Å, and it is not really possible to draw a line between bonded and non-bonded neighbours. Some molecules are linked to both barium atoms and to either or both of water molecules and oxygen atoms, others are not linked to barium atoms and have triangular coordination. In natrolite (Meier, 1960), the single water molecule has a curious one-sided coordination, being close to two oxygen atoms (2·9 Å) and two sodium atoms (2·4 Å); other oxygen atoms are at 3·3 Å and over. It may be seen from Fig. 5 that the coordinations of the water molecules in chabazite are complex and varied, which is not surprising in view of the patterns found in harmotome and natrolite.

To summarize this discussion it may be said that the balance of evidence favours the suggestion of a twinned triclinic structure for chabazite, but that the evidence is far from overwhelming. Other lines of attack are possible. Perhaps the most obvious is to search for a chabazite specimen with an intergrowth coarse enough to permit preparation of a single domain large enough for X-ray study. X-ray diffraction analysis would then yield a rigorous test of the proposed structure. If the structure were proved to be basically correct, it would be of importance to make an accurate 3D analysis in order to determine the details of the coordination of the Ca atoms and the water molecules. Other lines of attack might use neutron diffraction and proton magnetic resonance: for both, large single crystals would be necessary and the technical difficulties would be even more severe than for X-ray diffraction.

Finally it may be suggested that other zeolites may have a similar type of structure in which the morphology has a higher symmetry than the atomic positions. Steinfink (1962) has found that the en-

vironments of the cations and water molecules in phillipsite are as uncertain as those given here for chabazite; indeed it was not certain whether some peaks belonged to water molecules or to cations, and moreover H_2O–O distances as low as 1·8 Å were found. Steinfink assigned phillipsite to the orthorhombic system, but optical data (Winchell & Winchell, 1951) indicate lower symmetry, perhaps triclinic, while Wyart & Chatelain (1938) reported a monoclinic unit cell. It would not be surprising if phillipsite had a symmetry lower than orthorhombic so that the short interatomic distances in Steinfink's structure result merely from twinning of an ordered framework. Dr K. Fischer of Frankfurt has kindly informed me that he has found similar difficulties in locating the cations and water molecules in hydrated gmelinite, a zeolite with a similar structure to chabazite (Fischer, 1960; Dent & Smith, 1958). Winchell & Winchell (1951) record biaxial optical properties for this zeolite also even though the X-ray symmetry is hexagonal. Consequently the phenomena observed in chabazite do not appear to be unique in zeolites.

In conclusion it should be emphasized that, although the facts are consistent with a twinned, ordered, triclinic structure of chabazite, the conclusion is not as certain as would be desirable. Moreover there remains the possibility that chabazite is a variable mineral with both ordered and disordered types occurring. Although this would explain the different values of the optic axial angle quoted in the literature, there is the other possibility that all chabazites are ordered, and that the variable optical properties result merely from variable domain size.

References

ATOJI, M. & RUNDLE, R. R. (1958). *J. Chem. Phys.* **29**, 1306.

ATTARD, A. E. & AZAROFF, L. V. (1960). *J. Sci. Instrum.* **37**, 238.

DENT, L. S. & SMITH, J. V. (1958). *Nature, Lond.* **181**, 1794.

DEVIK, O., FINBAK, C. & RØNNING, O. (1944). *Tidsskr. Kemi Bergv.* **4**, 50.

DUCROS, P. (1960). *Bull. Soc. Franç. Minér. Crist.* **83**, 85.

FISCHER, K. (1960). *Fortschr. Min.* **38**, 201.

FISCHER, K. (1962). Personal communication.

HOWELL, P. A. (1960). *Acta Cryst.* **13**, 737.

MAJER, V. (1953). *Jugosl. Akad. Znanoski Umjetnoski,* p. 175.

MEGAW, H. D. (1952). *Acta Cryst.* **5**, 477.

MEGAW, H. D., KEMPSTER, C. J. E. & RADOSLOVICH, E. W. (1962). *Acta Cryst.* **15**, 1017.

MEIER, W. M. (1960). *Z. Kristallogr.* **113**, 430.

SADANAGA, R., MARUMO, F. & TAKÉUCHI, Y. (1961). *Acta Cryst.* **14**, 1153.

SMITH, J. V. (1962). *Acta Cryst.* **15**, 835.

SMITH, J. V. & BAILEY, S. W. (1963). *Acta Cryst.* **16**, 801.

SMITH, J. V., RINALDI, F. & GLASSER, L. D. (1963). *Acta Cryst.* **16**, 45.

STEINFINK, H. (1962). *Acta Cryst.* **15**, 644.

VAND, V., EILAND, P. F. & PEPINSKY, R. (1957). *Acta Cryst.* **10**, 303.

WELLS, A. F. (1962). *Structural Inorganic Chemistry.* Oxford Univ. Press.

WINCHELL, A. N. & WINCHELL, H. (1951). *Elements of Optical Mineralogy.* Part II. *Description of Minerals.* Fourth Edition. New York: Wiley.

WYART, J. & CHATELAIN, P. (1938). *Bull. Soc. Franç. Minér. Crist.* **61**, 121.

The Structure of Cleavamine: X-ray Analysis of Cleavamine Methiodide

BY NORMAN CAMERMAN AND JAMES TROTTER

Department of Chemistry, The University of British Columbia, Vancouver 8, B.C., Canada

The structure of the alkaloid cleavamine, $C_{19}H_{24}N_2$, has been determined by X-ray analysis of the methiodide, crystals of which are orthorhombic with four molecules in a unit cell of dimensions $a = 7.86$, $b = 14.86$, $c = 16.32$ Å, space group $P2_12_12_1$. The intensities of about 600 reflexions were measured on a G. E. spectrogoniometer, a scintillation counter and Mo $K\alpha$ radiation being used. The iodine atom position was determined by Patterson methods; x_I was close to $\frac{1}{4}$, but although this gave rise to false symmetry all the carbon and nitrogen atoms were located on three successive three-dimensional electron-density distributions, and all the positional and individual isotropic thermal parameters were then refined by four cycles of differential synthesis and six cycles of least squares. The final R value was 0.084. The absolute configuration was determined by the anomalous dispersion method.

The presence of the iodine atom prevents accurate measurement of the bond distances and valency angles, despite the excellent agreement between measured and calculated structure factor data, but the measurements are sufficiently precise to distinguish between the different types of bonds and angles. The indole nucleus and the two attached carbon atoms are planar; the two ethylenic carbon atoms and the three carbon atoms bonded to them also lie in one plane. A significant feature of the molecular packing is a N–H ⋯ I hydrogen bond of length 3.4 Å, involving the indole nitrogen atom.

Introduction

The study of the action of acidic reagents on some of the simpler alkaloids isolated from *Vinca rosea* Linn provides important information about the effect of such reagents on the biologically important alkaloids vincaleukoblastine and leurosine. The reaction of catharanthine (I) with concentrated hydrochloric acid yields two products, one of which is simply desmethoxycarbonylcatharanthine. The second product, cleavamine, $C_{19}H_{24}N_2$, involves more drastic rearrangement; analytical, ultraviolet, infrared and nuclear magnetic resonance data suggest a tetracyclic ring skeleton for cleavamine, with retention of the indole chromophore and ethylenic double bond, and loss of the ester function of catharanthine (Kutney, Trotter, Tabata, Kerigan & Camerman, 1963).

The present paper describes an X-ray analysis of cleavamine methiodide, which establishes the structure of the alkaloid, including the absolute configuration,

I

II
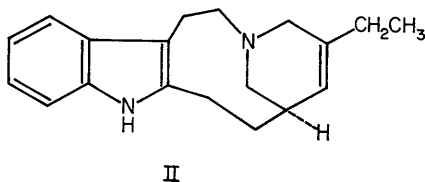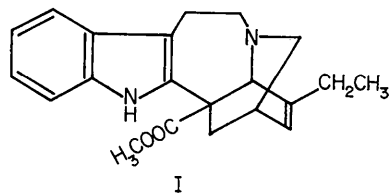
as (II). This formulation is in accord with all the chemical evidence.